





## Article

# Rheological Behavior and Characterization of Drinking Water Treatment Sludge from Morocco

Fantasse Azeddine <sup>1,\*</sup> , Parra Angarita Sergio <sup>1</sup> , Léonard Angélique <sup>1</sup> , Lakhel El Khadir <sup>2</sup>, Idlimam Ali <sup>3</sup> and Bougayr El Houssayne <sup>4</sup> 

<sup>1</sup> Chemical Engineering Research Unit, PEPs, University of Liège, 4000 Liège, Belgium

<sup>2</sup> Laboratory of Fluid Mechanics and Energetics (LMFE), Faculty of Sciences Semlalia, Cadi Ayyad University, Marrakesh 40000, Morocco

<sup>3</sup> Team of Solar Energy and Medicinal Plants EESPAM, Teacher's Training College, Cadi Ayyad University, Marrakesh 40000, Morocco

<sup>4</sup> Engineering & Applied Technologies Laboratory (LITA), Higher School of Technology—Beni Mellal, Sultan Moulay Slimane University, Beni-Mellal 23000, Morocco

\* Correspondence: azeddinefantasse@gmail.com

**Abstract:** Drinking water treatment generates a high amount of pasty by-product known as drinking water treatment sludge (DWTS). The chemical composition, microstructure and rheological behavior of DWTS are of utmost importance in the calculation, design, optimization, commissioning and control of its treatment processes. The purpose of this research was to characterize the DWTS from the drinking water treatment plant of Marrakech (Morocco), aiming to help future researchers and engineers in predicting its hydrodynamic behavior. The first part of this study was devoted to the physical structure and the chemical composition of sludge. The second part was oriented towards the study of the mechanical properties; a penetration test and a rotational rheology test were performed. For the first test, a force–length penetration diagram was plotted in order to calculate the hardness, the cohesiveness and the adhesiveness of DWTS. For the second test, the shear stress and the apparent viscosity were plotted and fitted to five rheological models, as function of the shear rate, aiming to describe the rheological behavior of samples. The obtained results reveal that the drinking water treatment sludge from Marrakech is a porous, amorphous and highly adhesive material, with a shear-thinning (pseudoplastic) rheological behavior that can be described according to the Herschel–Bulkley model (better in low-rate stresses,  $R^2 = 0.98$ ) or the Windhad model (better in high shear rates,  $R^2 = 0.96$ ) and is mainly composed of silica, aluminum and iron oxides.

**Keywords:** drinking water treatment sludge; rheology; texture; chemical characterization; waste management



**Citation:** Azeddine, F.; Sergio, P.A.; Angélique, L.; El Khadir, L.; Ali, I.; El Houssayne, B. Rheological Behavior and Characterization of Drinking Water Treatment Sludge from Morocco. *Clean Technol.* **2023**, *5*, 259–274. <https://doi.org/10.3390/cleantechnol5010015>

Academic Editors: Patricia Luis and Constantinos V. Chrysikopoulos

Received: 29 November 2022

Revised: 31 January 2023

Accepted: 3 February 2023

Published: 16 February 2023



**Copyright:** © 2023 by the authors. Licensee MDPI, Basel, Switzerland. This article is an open access article distributed under the terms and conditions of the Creative Commons Attribution (CC BY) license (<https://creativecommons.org/licenses/by/4.0/>).

## 1. Introduction

The treatment process of drinking water generates a high amount of a paste-like by-product; this material is referred to as ‘drinking water treatment sludge’ (DWTS) or ‘hydroxide sludge’ in the literature [1]. The chemical composition and physical characteristics of DWTS depend on its origin, the sampling season and the type of treatment applied [2]. This implies that there is not a single category of drinking water sludge, but a whole variety of different sludge materials.

The management of DWTS is a major challenge due to the increasing volumes, in addition to the potential threat to the environment and acute disposal issues [3,4]. In the drinking water production plant of Marrakech (Morocco) alone, 55 tons of DWTS are generated per day [5]. The influent to this plant is raw water, coming mainly from the Hassan I Dam reservoir.

DWTS has a gelatinous consistency and heterogeneous composition. DWTS is largely made up of inorganic compounds, mainly silicon oxides, aluminum oxides and iron oxides,

and its solid content can vary from 3 to 30% depending on the treatment [5]. The pH value of DWTS ranges between 6.2 and 7, depending on the season [3].

In general, DWTS has an amorphous and porous structure, which is formed by particles that are irregular in size and shape [1,5–7]. It is well-known that DWTS is a non-Newtonian fluid with shear-thinning (pseudoplastic) behavior, i.e., the viscosity of the material decreases under the effect of a shear stress load.

The precise prediction of the hydrodynamic behavior of the sludge is necessary for the calculation, design, commissioning and correct operation of different equipment, such as pumps, dryers, filtration systems, heat exchangers, mixing systems, etc. Predicting the correct flow behavior of these engineered hydrodynamic processes requires accurate knowledge of the chemical composition and mechanical (including rheological) characteristics of the DWTS [1,8–10].

Sludge is a muddy leftover material that might be solid, semisolid or liquid. The design of pumping systems, mixing, hydrodynamics and mass transfer rates of various sludge treatment units, as well as the optimization of conditioning dose and sustainable sludge management, all depend on an understanding of the flow behavior and rheological properties of sewage sludge at different sections of a drinking and wastewater treatment plant (WWTP) [11].

The characterization of the rheological properties of hydroxide sludges from DWTS represents one of the few examples of fundamentally derivable properties that has also been successfully linked to real sludge treatment processes. The rheological characterization of this type of sludge, which has never been studied, is of great importance for downstream treatment related to the optimized pumping and mixing of sludge, the evaluation of energy demands and the overall process [8,12,13]. However, working out a rheological behavior can later help in optimizing the dynamic operational conditions in practice [10,14].

The purpose of this experimental work is to characterize the drinking water treatment sludge (DWTS) from the drinking water treatment plant of Marrakech (Morocco), aiming to help future researchers and engineers in predicting the hydrodynamic behavior of the DWTS. This study is divided into two detailed parts. The first is dedicated to the physico-chemical analysis of hydroxide sludge. The second part of the current study consists in analyzing the texture properties of the hydroxide sludge as well as the different rheological models such as those of Ostwald–de Waele, Herschel and Bulkley, Bingham, Windhab and Casson to estimate indicators of the rheological behavior of DWTS.

## 2. Materials and Methods

### 2.1. Sludge Samples

The sludge samples used in this research came from the Marrakech drinking water treatment plant. In order to produce drinking water to supply the population of the city of Marrakech and surrounding centers, the plant has two treatment processes:

**Water treatment:** The treatment of water in the plant follows a classic process as shown in Figure 1, with the following succession of stages: Screening–De-sludging–Pre-chlorination–Coagulation/Flocculation–Decantation–Filtration–Post-chlorination. The reagents used to ensure the treatment are as follows: aluminum sulphate as the main coagulant, polyelectrolyte as a flocculation aid and chlorine gas to ensure oxidation and disinfection.

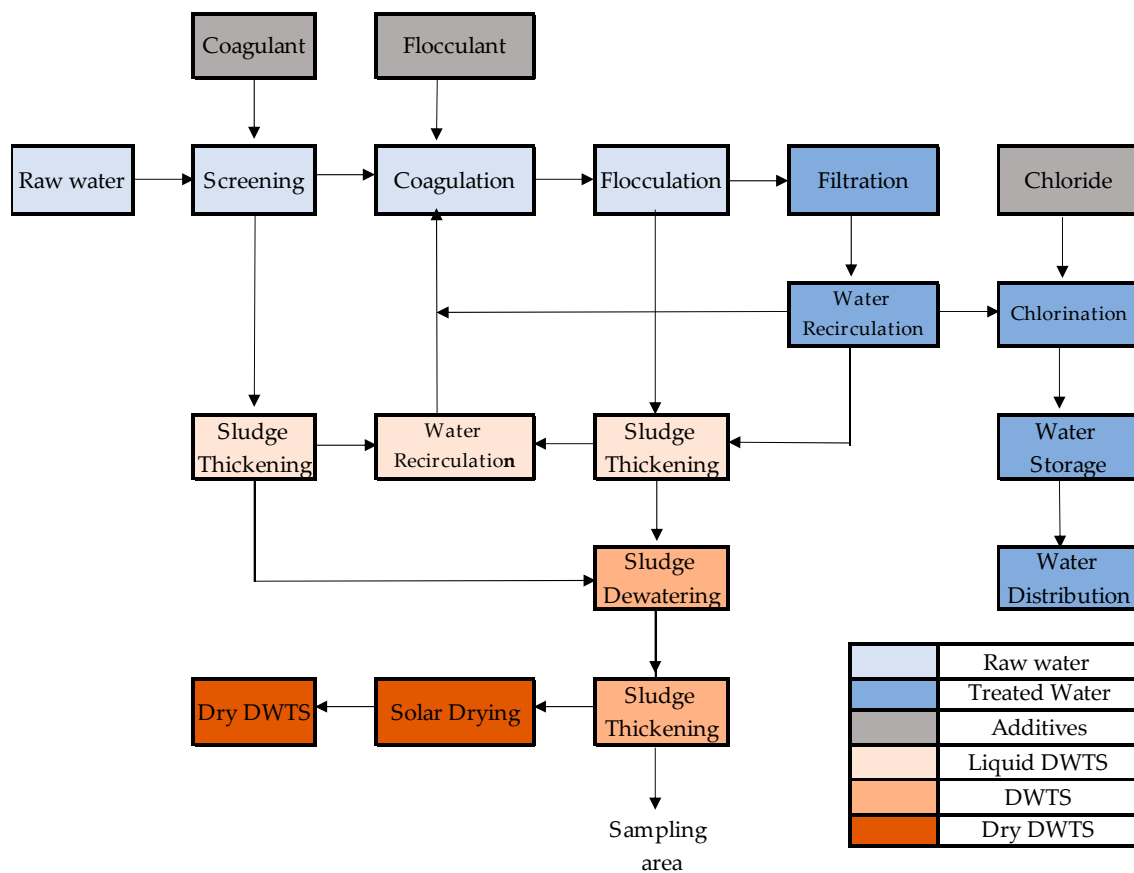


**Figure 1.** DWTS Production Plan in Marrakech.

The samples were taken from the sludge storage tank, in which the thickened and pressed sediment streams of the primary and secondary treatments and the back-washing of the filters converge; a picture of the sludge is shown in Figure 2.



**Figure 2.** DWTS Sample.

In order to define the chemical composition of DWTS and to supervise the effect of floods, which may appear in the rainy season, DWTS samples were taken during the wet season. After sampling, the samples were stored at 4 °C for the duration of the characterization time (4 weeks).

## 2.2. Chemical Composition and Characterization

### Chemical Characterization

The analysis of the chemical composition of DWTS by inductively coupled plasma atomic emission spectroscopy (ICP-AES) was conducted at the Marrakech drinking water treatment plant, using the methodology proposed by J. Rodier et al. [15]. The results for major components were expressed in percentages and, for minor components, in mg/kg.

Total solids content (TS) and the loss on ignition (LOI), also known as the volatile solids content of DWTS, were determined according to the standard methodology [16]. The DWTS samples were dried at 105 °C until mass stabilization, then we calcinated the dried residue at 550 °C for 2 h and weighed the samples.

### 2.3. Analysis by Scanning Electron Microscopy: SEM (EDX)

The scanning electron microscopy (SEM) analyses were conducted using a JEOL JSM-840A scanning microscope equipped with an Oxford ISIS 300 microanalysis system for energy-dispersive X-ray spectroscopy (EDX). The SEM was performed under the following conditions: probe current of 45 nA, acceleration voltage of 20 kV and counting time of 60 s, with online ZAF correction. The micrographs were obtained with 1000-times magnification.

### 2.4. Measurement of Textural Properties

The textural properties were measured using a LS1 penetrometer universal traction machine (AMETEK Lloyd Instruments, West Sussex, England), equipped with a 10 N probe and a 30 mm diameter spherical geometry probe. The samples were penetrated to a depth of 15 mm at a constant speed of 1 mm/s according to the methodology proposed by Hil et al. [17] and modified by Y. Pambou [18]. All measurements were performed at a controlled temperature of 20 °C.

A texture test is characterized by a cycle corresponding to a load phase (compression), a relaxation phase and a discharge phase (decompression) under the sample. During the measurement, the force applied and the distance traveled by the probe were recorded. A force–penetration diagram was plotted with the obtained data in order to calculate the hardness, cohesiveness and adhesiveness of the sample.

### 2.5. Rheological Characterization

The rheological behavior of sludge was measured using an MCR302e rotational rheometer (Anton Paar, Graz, Austria) equipped with 50 mm diameter serrated parallel plate geometry. The equipment was controlled with Rheocompas 1.30 software. All measurements were performed at a controlled temperature of 20 °C to minimize the evaporation of moisture from the samples, and only the steady stable mode of the equipment was used.

The flow curve and the viscosity curve of the sample were measured using a gap of 1 mm, a shear rate range from 0.01 to 100 [1/s] and a controlled temperature equal to 20 °C. The measurement conditions were chosen from previous research conducted on similar materials [9].

The fitting of the results was established with five commonly used rheological models in order to analyze the dependence of the shear stress ( $\tau$ ) on the shear rate ( $\dot{\gamma}$ ) and to describe the pasty materials; these models included the Ostwald–de Waele (or power law) model (Equation (1)), Herschel–Bulkley model (Equation (2)), Casson model (Equation (3)), Bingham–Papanastasiou model (Equation (4)) and Windhab model (Equation (7)). Table 1 contains the equations of the models and definitions of their parameters.

**Table 1.** Rheological models used to describe hydroxide sludge rheology.

Rheological Model	Equation			Description
Ostwald–de Waele	$\tau = k\dot{\gamma}^n$	(1)	$k$ $n$	Consistency coefficient [Pa·s <sup>n</sup> ] Rate index
Herschel–Bulkley	$\tau = \tau_0 + k\dot{\gamma}^n$	(2)	$\tau_0$ $k$ $n$	Yield point [Pa] Consistency coefficient [Pa·s <sup>n</sup> ] Rate index
Casson	$\sqrt{\tau} = \sqrt{\tau_c} + \sqrt{\eta_c \dot{\gamma}}$	(3)	$\tau_c$ $n_c$	Yield point [Pa] Plastic viscosity [Pa·s]
Bingham–Papanastasiou	$\tau = \eta \dot{\gamma} + \tau_0 \left(1 - e^{(-m\dot{\gamma})}\right)$	(4)	$\tau_0$ $n$ $m$	Yield point [Pa] Viscosity [Pa·s] Papanastasiou constant
Windhab	$\tau = \tau_0 + \eta_\infty \dot{\gamma} + (\tau_1 - \tau_0) \left(1 - e^{(-\frac{\dot{\gamma}}{\dot{\gamma}^*})}\right)$	(5)	$\tau_0$ $\tau_1$ $n_\infty$ $\dot{\gamma}^*$	Yield point [Pa] Shear stress [Pa] Steady-state viscosity [Pa·s] Windhab shear stress [s <sup>-1</sup> ]

The parameter estimation for all the models was conducted following the methodology proposed by T. G. Mezger [19]. In order to find the most suitable model for the experimental data, the coefficient of determination (R<sup>2</sup>) was calculated to evaluate the models' predictive capability.

### 3. Results and Discussions

#### 3.1. Chemical Composition of DWTS

The chemical characterization of DWTS by ICP-AES shows that the samples' major components were SiO<sub>2</sub>, Al<sub>2</sub>O<sub>3</sub> and Fe<sub>2</sub>O<sub>3</sub> as shown in Table 2. As mentioned before, DWTS chemical composition changes depending on its origin; nonetheless, these three compounds have major quantities in the composition of DWTS (not always in the same hierarchical order). Table 2 shows some chemical characterization results of the DWTS discussed in this study and other DWTS sludges from different countries.

**Table 2.** Major Chemical composition of DWTS from different countries.

Parameter	Unit	DWTS Origin					
		Marrakech (Morocco) (Current Sludge)	Ghaziabad (India) [6]	Barcelona (Spain) [20]	Adelaide (Australia) [21]	Sungai Dua Penang (Malaysia) [22]	Rabat (Morocco) [23]
SiO <sub>2</sub>		44.8 ± 0.86	52.78	29.63	26.43	40.33	27.12
Al <sub>2</sub> O <sub>3</sub>	wt%	26.1 ± 0.48	14.38	17.57	28.27	31.84	62.66
Fe <sub>2</sub> O <sub>3</sub>		8 ± 0.18	5.20	5.18	6.66	6.43	1.16

A comparison with the chemical characterization of a sample of pure clay shows that DWTS composition is similar in proportion, with the only exception being aluminum oxide content, the excess of which essentially comes from its addition during processing [13].

The content of other major components such as calcium, magnesium, titanium and potassium oxides, minor components and also those that are not figured (NF) in DWTS are shown in Table 3. The confidence intervals for each value of the major and minor components constituting the sludge are given.

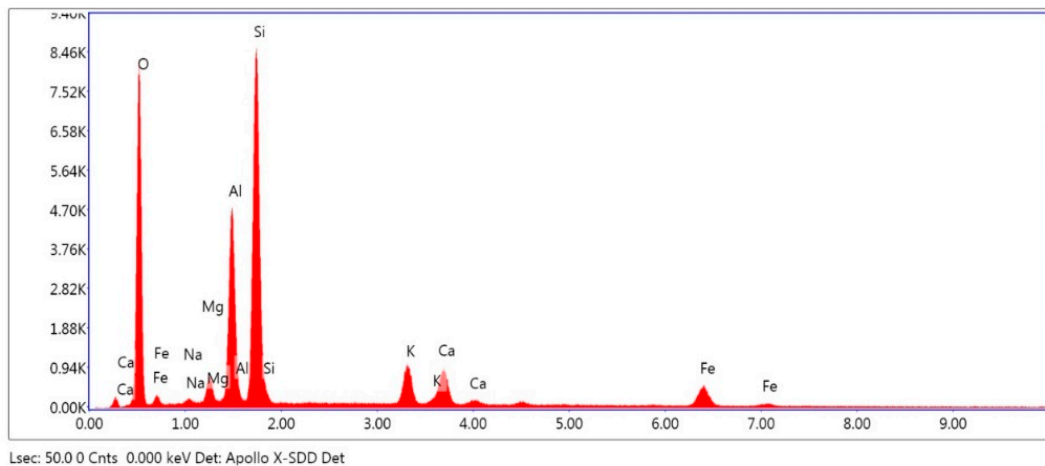
**Table 3.** Chemical composition of DWTS from Marrakech (Wet season).

Majority Composition		Minority Composition			
Parameter	wt%	Parameter	mg/kg	Parameter	mg/kg
CaO	4 ± 0.39	Ba	693 ± 22	Nb	42 ± 6
MgO	3.8 ± 0.26	As	179 ± 6	Mo	16 ± 3
K <sub>2</sub> O	4 ± 0.06	Cr	153 ± 17	Cd	13 ± 1
MnO	0.16 ± 0.02	Li	127 ± 16	Be	5 ± 0.52
TiO	0.8 ± 0.14	B	123 ± 10	Se	NF
		Sb	83 ± 14	Bi	NF
		Sn	44 ± 2	Ge	NF
		Cu	56 ± 17		
		Co	53 ± 10		

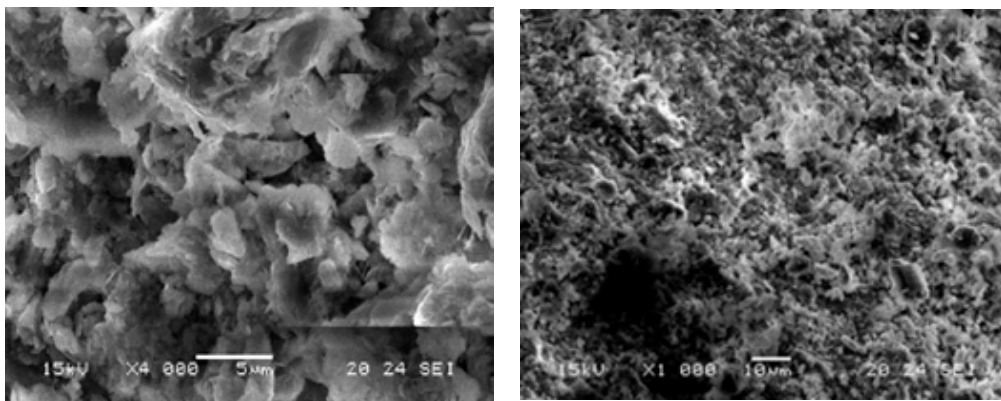
The presence of volatile matter content is an important criterion for sludge characterization. The total solid content was 25.41% (wet basis) and the volatile matter content (LOI) was 18.47% (dry basis). The volatile matter content in the sludge sample was low, with a content lower than 30%, which makes the sludge easy to dewater and thicken.

### 3.2. Analysis by Scanning Electron Microscopy: SEM (EDX)

The microstructure of the sample characterized by the presence of micropores explains the adsorbent power of the material studied. The micrographs obtained with 1000-times magnification show the heterogeneity of their structure (Figure 3b,c). The presence of micropores explains the nature and the size of the constituents of the analyzed sample. Generally, these constituents are of a sandy nature, which is explained by the presence of granular phases of important size.



(a)



(b): 4000× magnification

(c): 1000× magnification

**Figure 3.** (a) Mass percentage of minerals contained in the hydroxide sludge; (b,c) Micrograph analysis of the hydroxide sludge.

The analysis of the sludge by SEM-EDX showed that the sludge is composed mainly of silica, aluminum and iron oxides, which correlates well with the main mineral composition revealed by the ICP method.

### 3.3. Texture Measurements Results

In Figure 4, the penetration curve for hydroxide sludge samples is shown (mean curve for three replicates). In this graphic, the maximum positive peak ( $F_{max}$  in N) corresponds to the force necessary for the probe to penetrate the sample to the maximum depth;  $F_{max}$  is generally assimilated to the sample's firmness or hardness parameter. The positive area ( $A+$  in mJ/Nmm) under the curve up to  $F_{max}$  corresponds to the work carried by the probe during the compression test on the product. The minimum negative peak ( $F_{min}$  in N) is the force required to separate the sample from the probe.  $F_{min}$  is defined as the adhesive force of the sample; the more this force is negative, the more the product is adhesive. The negative area ( $A-$ , mJ/Nmm) under the curve is the work needed to detach the probe from the sample;  $A-$  is likened to an adhesiveness, stickiness or tackiness index (energy required to remove the sample from surfaces) [17].

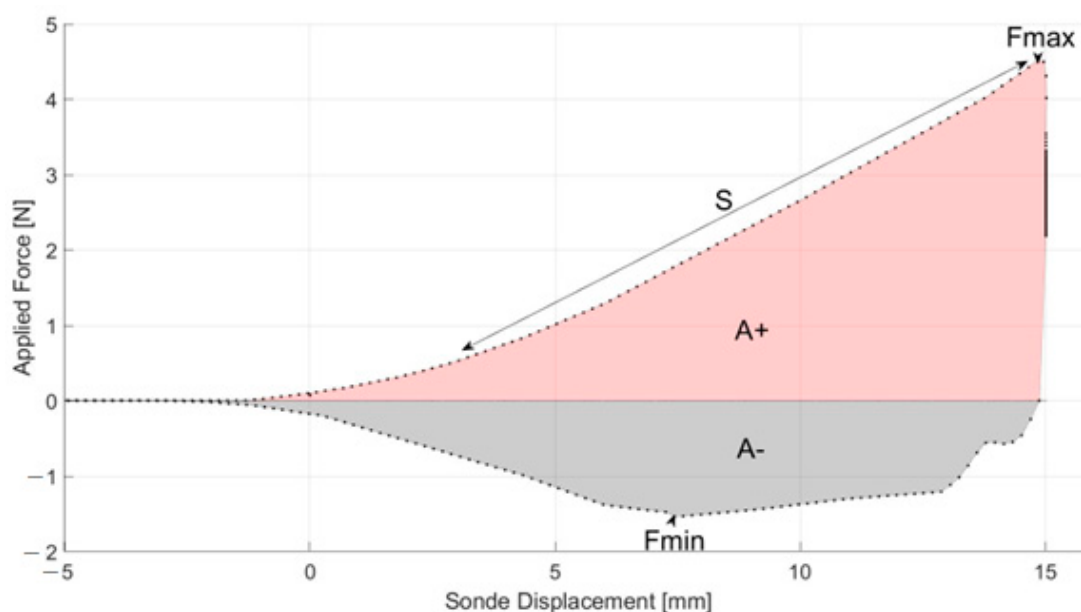


**Figure 4.** Experimental penetration curve for hydroxide sludge.

The initial slope of the positive part of the penetration curve ( $S$  in  $N/mm$ ) is related to the rigidity of the sludge sample [20]. Finally, the cohesive load of the sample was obtained from the maximum load value recorded (in  $kPa$ ) when the probe penetrates the sample [18]. The mean values for the textural properties of DWTS are given in Table 4 (mean of three measurements).

**Table 4.** Textural properties of hydroxide sludge.

Parameter	Unit	Value
Hardness	N	$4.843 \pm 0.173$
Hardness Work performed (mJ)	mJ	$29.606 \pm 1.646$
Adhesive force	N	$-1.607 \pm 0.062$
Adhesiveness	mJ	$21.480 \pm 1.266$
Rigidity	$N/mm$	$0.335 \pm 0.030$
Cohesive load	$kPa$	$6.834 \pm 0.244$

The mean values of the textural parameters for DWTS are not reported in the literature; however, the results obtained in this investigation have the same order of magnitude as those found for sewage sludge samples after and before liming [24].

### 3.4. DWTS Rheological Characteristics

In order to investigate and describe the rheological behavior of DWTS, the mean values (three replicates) of shear stress (flow curve or rheogram) and apparent viscosity were plotted as a function of shear rate in Figures 4a and 4b, respectively.

As depicted in Figure 5a, the DWTS possessed a non-linear relationship between shear stress and shear rate, which indicates non-Newtonian behavior of the sample. The changes in the flow curve (Figure 5a) are related with different structural changes in DWTS during the shear process. In this plot, three regions can be identified: Region 1 represents the measured yield point or yield stress, i.e., the applied stress at which irreversible plastic deformation is first observed across the sample [25]. The existence yield point was obtained using the methodology proposed by B. Clercq, applying zoom-in at low shear rates [26]. Region 2 represents the intermediate flow region, which describes



the shear-induced structure, and finally, Region 3 represents the flow function in the high shear region, whereby the shear stress increased non-linearly with shear rate, indicating non-Newtonian fluid behavior [9,27,28].

The apparent viscosity of DWTS at the beginning of the test (lowest shears rates) dropped dramatically, and then tended to a relatively constant value (highest shears rates) (Figure 5b). During this process, sludge tended to be less viscous, demonstrating shear-thinning (pseudoplastic) behavior. Similar rheological behaviors have been reported for sewage sludge [9], ink [27], foam [27], clay [29], paint [30] and chocolate [30], among others [30,31].

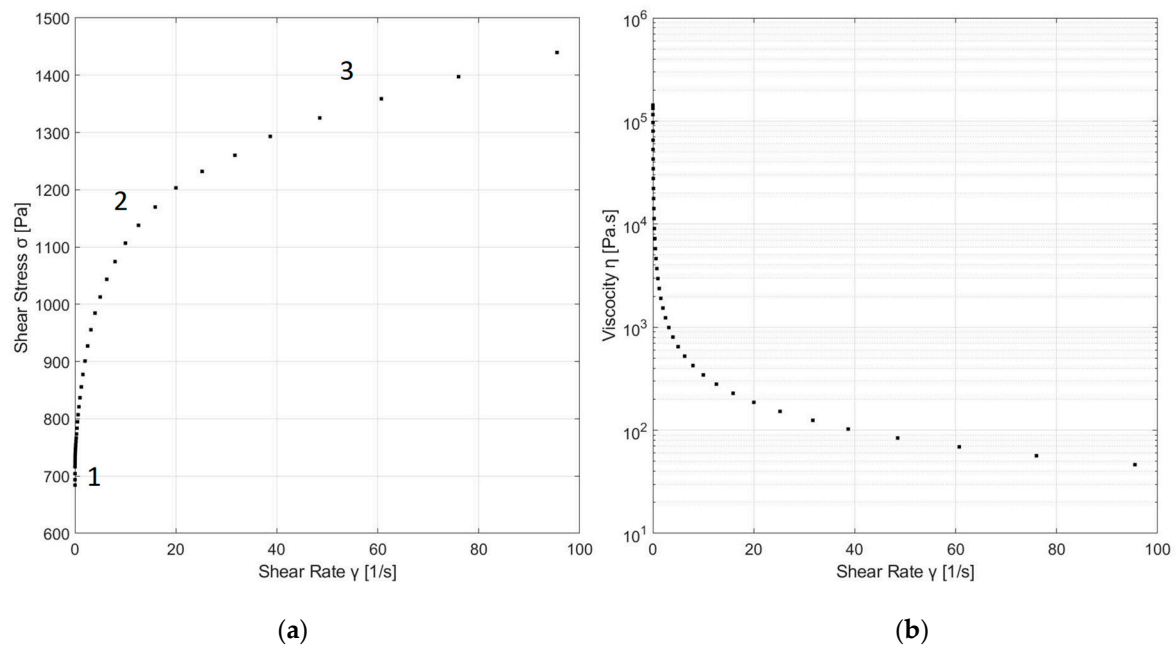


**Figure 5.** (a) Experimental flow curve for hydroxide sludge and (b) Apparent viscosity as a function of shear rate.

### 3.5. DWTS Rheological Modeling

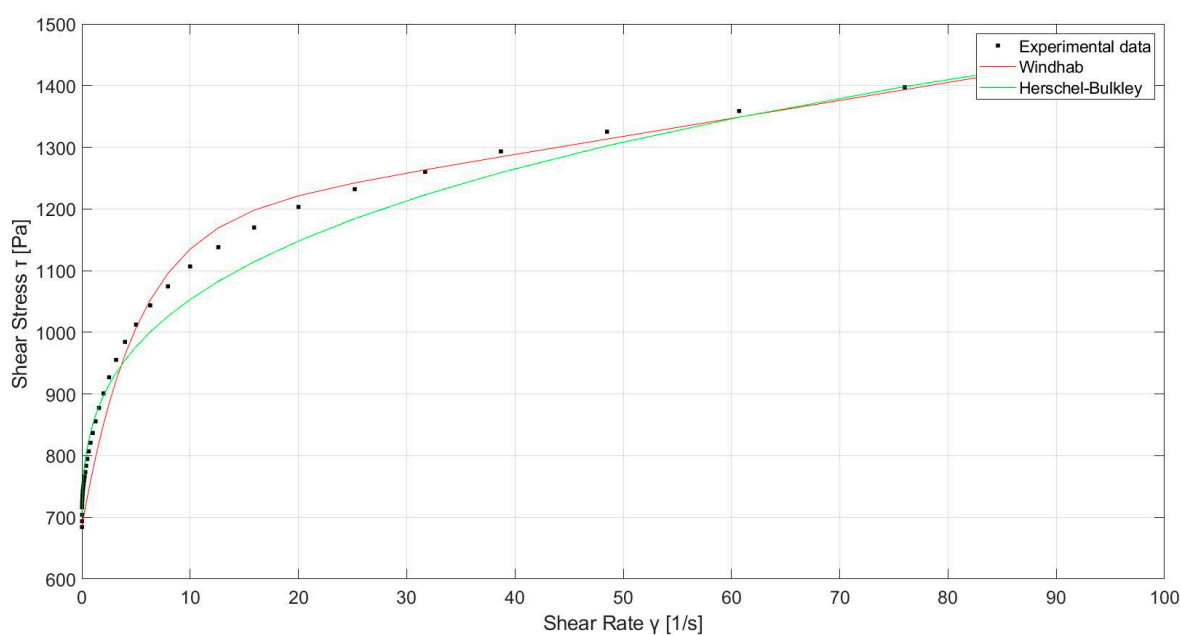
Aiming to understand the rheological behavior of DWTS, the experimental flow curve was fitted to five different rheological models commonly used to describe pasty materials. Table 5 contains the results of the fitting of experimental data.

**Table 5.** Identification of the parameters of the rheological used models for DWTS.

Rheological Model	Parameters Values	R <sup>2</sup>
Ostwald–de Waele	$k = 910 \pm 15 \text{ Pa}\cdot\text{s}^n$ $n = 0.08 \pm 0.01$	0.94
Herschel–Bulkley	$\tau_0 = 653 \pm 28 \text{ Pa}$ $k = 197 \pm 30 \text{ Pa}\cdot\text{s}^n$ $n = 0.3 \pm 0.07$	0.98
Casson	$\tau_c = 752 \pm 23 \text{ Pa}$ $n_c = 1.8 \pm 0.01 \text{ Pa}\cdot\text{s}$	0.91
Bingham–Papanastasiou	$\tau_0 = 1184 \pm 400 \text{ Pa}$ $n = 3 \pm 9 \text{ Pa}\cdot\text{s}$ $m = 1 \pm 0.3$	<0.00
Windhab	$\tau_0 = \pm 23 \text{ Pa}$ $\tau_1 = 1172 \pm 42 \text{ Pa}$ $n_\infty = 3 \pm 0.8 \text{ Pa}\cdot\text{s}$ $\dot{\gamma}^* = 5 \pm 1 \text{ s}^{-1}$	0.96

All the fitted models to the experimental data showed coefficient of determination values greater than 0.9, except for the Bingham–Papanastasiou (BP) model, which obtained an R<sup>2</sup> less than zero. The obtained parameters have an enormous confidence interval (bigger than the proposed parameter value), i.e., a horizontal line better fits the experimental data than this model. This is possibly due to the fact that the studied sample has characteristics of a plastic fluid, as is shown in the previous section (yield stress existence), and the BP model is a modification of the Bingham model (ideal plastic) for fluids without a yield point.

The coefficient of determination values in Table 5 revealed that the Herschel–Bulkley (R<sup>2</sup> = 0.98) and Windhab (R<sup>2</sup> = 0.96) models accurately describe the flow behavior of the samples. However, as seen in Figure 6, the two models fit better in different ranges of shear rate, with the Herschel–Bulkley model fitting better at shear rates lower than 1 s<sup>-1</sup> (Figure 6b) and the Windhab model at shear rates higher than 10 s<sup>-1</sup> (Figure 6c).



(a)

**Figure 6.** Cont.

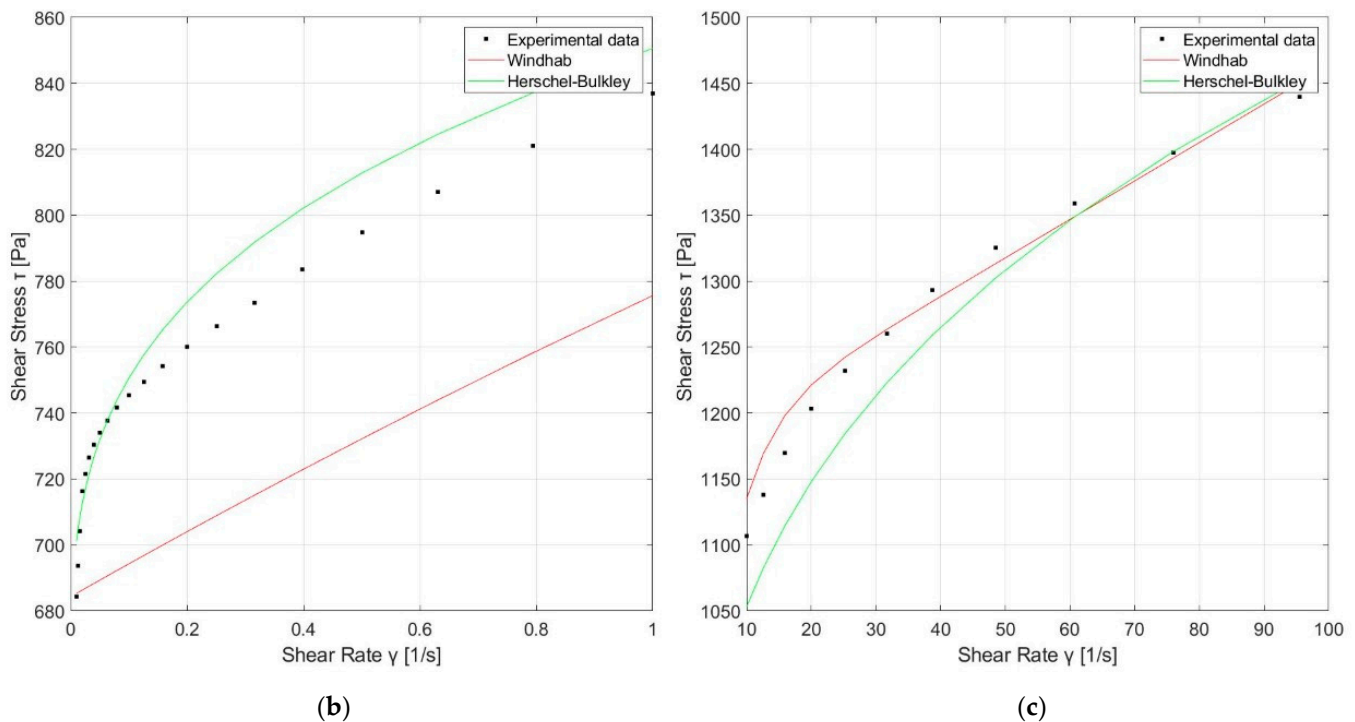


**Figure 6.** Experimental flow curve for hydroxide sludge fitted to Herschel–Bulkley and Windhab models for (a) all shear rate, (b) lower shear rates ( $\dot{\gamma} < 1 \text{ s}^{-1}$ ) and (c) higher shear rates ( $\dot{\gamma} > 10 \text{ s}^{-1}$ ).

The Herschel–Bulkley model has been used to describe and model the yield strength behavior as a function of shear rate of sewage sludge [32] and clay [33] with high precision between 1 to 100  $\dot{\gamma} = 0.01$  to 100  $\text{s}^{-1}$ . These two last materials are similar in composition and structure to DWTS, so the value of the correlation coefficient obtained for this model is not a surprise. In contrast, the Windhab model is usually used to describe the rheological behavior of concentrated chocolate [34]; nevertheless, some authors have successfully used this model to adjust rheological data of different materials such as food (ketchup, sauces, mayonnaise, yogurt, margarine, etc.), sand, cement, ink and other pasty materials for shear rates between 1 to 100 ( $\dot{\gamma} = 1$  to 100  $\text{s}^{-1}$ ) [27,35], but it has been never used to describe the rheology of DWTS. Due to the reasons outlined above, the authors encourage future researchers to make use of the results for the Herschel–Bulkley model for future calculations.

### 3.6. Example Problem for Pumping of DWTS

The objective of this example problem is to show the variation obtained by using the rheological model (Case 1) and common assumptions (Case 2) in determining the power required by a pump to transport a mass flow of 55 ton/d of DWST through the diagram of the assembly line shown in Figure 7.

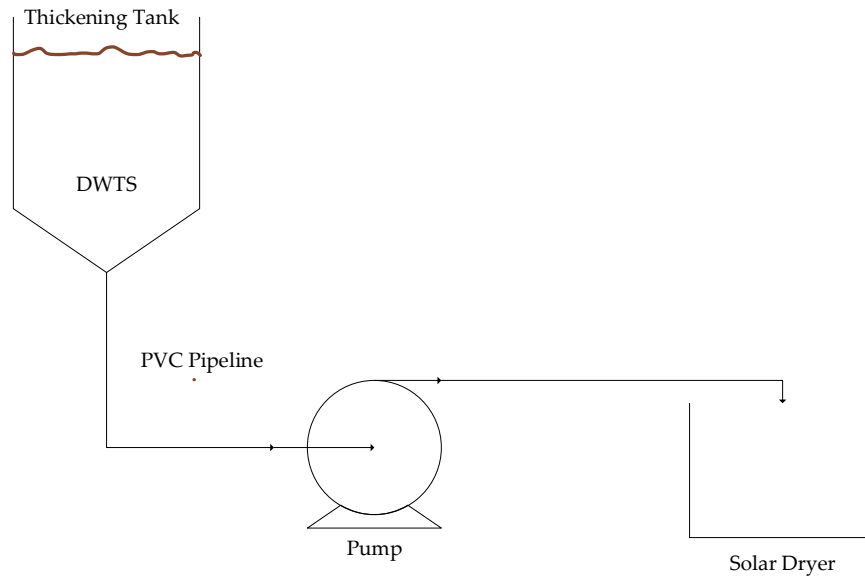


**Figure 7.** Schematic diagram of the assembly line.

The information necessary for the development of this problem is shown in Table 6. Calculations were performed using the methodology proposed by Garcia and Steffe [36].

**Table 6.** Data for example problem.

Data Type	Variable	Value
DWTS properties	Rate index	$n = 0.3$
	Consistency coefficient	$k = 197 \text{ Pa}\cdot\text{s}^n$
	Yield point	$\tau_o = 653 \text{ Pa}$
	Density	$\rho = 2200 \frac{\text{kg}}{\text{m}^3}$
	Viscosity	$\mu_\infty = 15 \text{ Pa}\cdot\text{s}$
Pumping system parameters	Mass flow	$\dot{M} = 0.64 \frac{\text{kg}}{\text{s}}$
	Pipe length	$L = 90 \text{ m}$
	Pipe diameter	$D = 0.1 \text{ m and } 0.2 \text{ m}$
	Accessories load loss	$\sum K = 2$
	Pump efficiency	$E = 0.7$
	Elevation change	$\Delta Z = 20 \text{ m}$
	Pressure drop	$\Delta P = -107.8 \text{ Pa}$

The work per unit mass required to pump an incompressible fluid through a pipe system is given by the mechanical energy balance equation.

$$W = F + \frac{\Delta P}{g} + g\Delta Z + \Delta K \quad (6)$$

The total energy loss due to friction ( $F$ ) can be written in terms of the Fanning equation and the summation of the energy loss in fittings and other devices in the line as

$$F = \frac{2fV^2L}{D} + \frac{\sum KV^2}{2} \quad (7)$$

The mass average velocity is

$$V = \frac{4M}{\pi\rho D^2} \quad (8)$$

Substituting Equations (7) and (8) into Equation (6) and assuming negligible kinetic energy change gives

$$W = \frac{32fM^2L}{\pi^2\rho^2D^5} + \frac{8M^2}{\pi^2\rho^2D^4} \sum K + \frac{\Delta P}{\rho} + g\Delta Z \quad (9)$$

where  $f$  is the frictional pressure drop for laminar flow conditions, which can be calculated as shown in Equation (10) for a Herschel–Bulkley fluid and as shown in Equation (11) for a Newtonian fluid.

$$f = \frac{16}{Re\Psi} \quad (10)$$

$$f = \frac{16}{Re} \quad (11)$$

where  $Re$  is the generalized Reynolds number (by definition),

$$Re = \frac{\rho D^n V^{2-n}}{8^{(n-1)}k} \left( \frac{4n}{1+3n} \right)^n \quad (12)$$

$$Re = \frac{4\rho M}{\pi D \mu_\infty} \quad (13)$$

Furthermore,

$$\Psi = (1+3n)^n (1-\xi)^{1+n} \left( \frac{(1-\xi)^2}{1+3n} + \frac{2\xi(1-\xi)}{1+3n} + \frac{\xi^2}{1+n} \right) \quad (14)$$

where  $\xi$ , the dimensionless unsheared plug radius, is

$$\xi = \frac{\tau_o}{0.5f\rho V^2} \quad (15)$$

To calculate the friction factor,  $\xi$  is estimated through iteration of the last three equations. Then,  $f$  can be calculated. Solving the equation system, we obtain the power requirement of the pump. The results for the two cases are shown in Table 7.

**Table 7.** Energy requirements for the pumping system.

Diameter (cm)	Power Requirement (kW)	
	Case 1	Case2
10	5.79	2.80
20	2.44	0.37

From the obtained results obtained for the two hypothetical scenarios (diameters of 10 and 20 cm), it can be deduced that by assuming that the DWTS is a Newtonian fluid, a lower power requirement is always obtained compared to that obtained when the calculations are carried out rigorously, using the rheological model proposed by the authors. In real life, undersizing a pump results in a lower-than-required flow rate in the system. This requires additional pumps or system adjustments, such as opening discharge valves and adding recirculation lines, increasing material transportation costs.

With a simple example, it was shown how the use of the found rheological model can be used to calculate the power of a pump; similarly, the procedure can be adapted to calculate equipment and operations for mixing, agitation, etc.

#### 4. Conclusions

In this paper, we have shown that the drinking water treatment sludge from Marrakech is mainly composed of silica, aluminum and iron oxides, with a porous and amorphous

microstructure. In addition, we found that this sludge has similar textural properties to that of sewage sludge. Finally, we proved that the DWTS is a shear-thinning (pseudoplastic) fluid; for shear stresses under the yield point, the material stays as a viscoelastic solid, and for stresses higher than the yield point, the sludge behaves as a yield stress fluid that can be modelled using Windhab (more accurate in low shear rates) and Herschel–Bulkley (more accurate in high shear rates) models over a wide range of shear rates.

This work allowed a characterization of drinking water treatment sludge for the understanding of the mechanisms involved in hydroxide sludge. The results showed in this paper will improve the calculation, design, optimization, commissioning and control of sludge treatment processes.

The knowledge of the chemical composition of DWTS provides a prediction of the stability and chemical reactivity of the material; this can be used to guarantee the optimal selection of the manufacturing material of different equipment and units that will have to make contact with DWTS, such as dryers, pipes, tanks, etc. Likewise, information given regarding textural characteristics and chemical characterization can be used to determine whether or not the sludge is suitable to be used as raw material in the manufacturing of different products (such as bricks or blocks), for the cogeneration of energy or for landfilling. Finally, the rheological results obtained showed that the fitted rheological models or the viscosity curve can be used for the calculation of the pressure drop in a pipeline that transports DWTS from the storage tank to a dryer or other equipment.

However, future researchers should prove whether the microstructure of DWTS and its textural and rheological behavior are similar or identical at different total solids content, in order to obtain a complete characterization of this material.

**Author Contributions:** Conceptualization, F.A., L.A. and P.A.S.; data curation, F.A. and P.A.S.; formal analysis, F.A. and P.A.S.; funding acquisition, F.A.; investigation, F.A. and P.A.S.; methodology, F.A., L.A. and P.A.S.; software, P.A.S.; supervision, L.A., L.E.K. and I.A.; visualization, B.E.H., L.E.K. and I.A.; writing—original draft, F.A., L.A. and P.A.S.; writing—review and editing, F.A., L.A., P.A.S. and L.E.K. All authors have read and agreed to the published version of the manuscript.

**Funding:** This work was supported by the Fund for Scientific Research (F.R.S.–FNRS) [T.0159.20-PDR].

**Institutional Review Board Statement:** Not applicable.

**Informed Consent Statement:** Not applicable.

**Data Availability Statement:** Not applicable.

**Acknowledgments:** The authors acknowledge the support of the Chemical Engineering Halle personal. The authors acknowledge the FRS-FNRS, Fund for Scientific Research, for a Research Project, grant T.0159.20-PDR.

**Conflicts of Interest:** The authors declare no conflict of interest.

## References

1. Benlalla, A.; Elmoussaouiti, M.; Cherkaoui, M.; Ait Hsain, L.; Assafi, M. Characterization and valorization of drinking water sludges applied to agricultural spreading. *J. Mater. Environ. Sci.* **2015**, *6*, 1692–1698.
2. Chahid, L.; Yaacoubi, A.; Bacaoui, A.; Lakhal, E. Valorization of drinking water treatment sludge (DWTS): Characterization and applications as coagulant and sorbent for Olive Mill Wastewater (OMW). *J. Mater. Environ. Sci.* **2015**, *6*, 2520–2533.
3. Azeddine, F.; El Khadir, L.; Ali, I. Thermodynamic Analysis and Mathematic Modeling of Waste Sludge from Drinking Water Treatment Plants. *J. Ecol. Eng.* **2022**, *23*, 140–149. [[CrossRef](#)]
4. Fantasse, A.; Lakhal, E.K.; Idlimam, A.; Kouhila, M.; Berroug, F.; El Haloui, Y. Management of hydroxide sludge waste using hygroscopic gravimetric method and physico-chemical characterization. *Mater. Today Proc.* **2020**, *27*, 3021–3027. [[CrossRef](#)]
5. Azeddine, F.; El Khadir, L.; Ali, I.; Fatiha, B. Energy efficiency of drying kinetics process of hydroxide sludge wastes in an indirect convection solar dryer. *J. Sol. Energy Eng.* **2021**, *143*, 041007. [[CrossRef](#)]
6. Ahmad, T.; Ahmad, K.; Alam, M. Characterization of Water Treatment Plant's Sludge and its Safe Disposal Options. *Procedia Environ. Sci.* **2016**, *35*, 950–955. [[CrossRef](#)]
7. Fudholi, A.; Otman, M.Y.; Ruslan, M.H.; Yahya, M.; Zaharim, A.; Sopian, K. Techno-Economic Analysis of Solar Drying System for Seaweed in Malaysia. In Proceedings of the 7th IASME/WSEAS International Conference on Energy, Environment, Ecosystems and Sustainable Development, Angers, France, 17–19 November 2011; pp. 89–95.
8. Hasar, H.; Kinaci, C.; Ünlü, A.; Toğrul, H.; Ipek, U. Rheological properties of activated sludge in a SBR. *Biochem. Eng. J.* **2004**, *20*, 1–6. [[CrossRef](#)]
9. Markis, F.; Baudez, J.C.; Parthasarathy, R.; Slatter, P.; Eshtiaghi, N. Rheological characterisation of primary and secondary sludge: Impact of solids concentration. *Chem. Eng. J.* **2014**, *253*, 526–537. [[CrossRef](#)]
10. Baroutian, S.; Eshtiaghi, N.; Gapes, D.J. Rheology of a primary and secondary sewage sludge mixture: Dependency on temperature and solid concentration. *Bioresour. Technol.* **2013**, *140*, 227–233. [[CrossRef](#)]
11. Hong, E.; Yeneneh, M.; Sen, K.; Ang, H.M.; Kayaalp, A. Accepted Manuscript A comprehensive review on rheological studies of sludge from various sections of municipal wastewater treatment plants for enhancement of process performance. *Adv. Colloid Interface Sci.* **2018**, *257*, 19–30. [[CrossRef](#)]
12. Guibaud, G.; Dollet, P.; Tixier, N.; Dagot, C.; Baudu, M. Characterisation of the evolution of activated sludges using rheological measurements. *Process Biochem.* **2004**, *39*, 1803–1810. [[CrossRef](#)]
13. Azeddine, F.; El Khadir, L.; Ali, I. Experimental Investigation of Solar Greenhouse Drying of Hydroxide Sludge under Summer and Winter Climate. *Polish J. Environ. Stud.* **2022**, *31*, 1–12. [[CrossRef](#)] [[PubMed](#)]
14. Eshtiaghi, N.; Markis, F.; Yap, S.D.; Baudez, J.C.; Slatter, P. Rheological characterisation of municipal sludge: A review. *Water Res.* **2013**, *47*, 5493–5510. [[CrossRef](#)] [[PubMed](#)]
15. Rodier, J.; Legube, B.; Merlet, N.; Régis, B. *L'analyse de l'eau*, 10th ed.; Dunod: Malakoff, France, 2016.
16. Dayton, E.; Research, N.B.-W.E. Characterization of drinking water treatment residuals for use as a soil substitute. *Wiley Online Libr.* **2001**, *73*, 52–57. [[CrossRef](#)]
17. Hil, A.; Judenne, E.; Remy, M. The effect of lime treatment on sludge rheological properties. *Technology* **2005**, *59*, 1–6.
18. Pambou, Y.-B. Influence du Conditionnement et de la Déshydratation Mécanique sur le Séchage des Boues D'épuration. Ph.D. Thesis, Université de Liège, Liège, Belgium, 2016.
19. Mezger, T. *The Rheology Handbook*; European Coatings: Hanover, Germany, 2020; ISBN 9783866306509.
20. Rodríguez, N.H.; Ramírez, S.M.; Varela, M.T.B.; Guillem, M.; Puig, J.; Larrotcha, E.; Flores, J. Re-use of drinking water treatment plant (DWTP) sludge: Characterization and technological behaviour of cement mortars with atomized sludge additions. *Cem. Concr. Res.* **2010**, *40*, 778–786. [[CrossRef](#)]
21. Liu, Y.; Zhuge, Y.; Chow, C.W.K.; Keegan, A.; Li, D.; Pham, P.N.; Huang, J.; Siddique, R. Utilization of drinking water treatment sludge in concrete paving blocks: Microstructural analysis, durability and leaching properties. *J. Environ. Manag.* **2020**, *262*, 110352. [[CrossRef](#)]
22. Ling, Y.P.; Tham, R.H.; Lim, S.M.; Fahim, M.; Ooi, C.H.; Krishnan, P.; Matsumoto, A.; Yeoh, F.Y. Evaluation and reutilization of water sludge from fresh water processing plant as a green clay substituent. *Appl. Clay Sci.* **2017**, *143*, 300–306. [[CrossRef](#)]
23. Benlalla, A.; Elmoussaouiti, M.; Dahhou, M.; Assafi, M. Utilization of water treatment plant sludge in structural ceramics bricks. *Appl. Clay Sci.* **2015**, *118*, 171–177. [[CrossRef](#)]
24. Dignac, M.; Ginestet, P.; Rybacki, D.; Bruchet, A.; Urbain, V.; Scribe, P. Fate of wastewater organic pollution during activated sludge treatment: Nature of residual organic matter. *Water Res.* **2020**, *34*, 4185–4194. [[CrossRef](#)]
25. AMETEK Scientific Instrumets. *Texture Analysis Application Notes*; AMETEK Scientific Instrumets: Berwyn, PA, USA, 2020.
26. DE Clercq, B. Computational Fluid Dynamics of Settling Tanks: Development of Experiments and Rheological, Settling, and Scraper Submodels. Ph.D. Thesis, Rijksuniversiteit te Gent, Ghent, Belgium, 2003.
27. Wang, Y.; Yang, W.; Wang, Q.; Liu, K.; Wang, C.; Chang, Q. The rheological performance of aqueous ceramic ink described based on the modified Windhab model. *Mater. Res. Express* **2020**, *7*, 75103. [[CrossRef](#)]
28. *TA Instruments Rheological Techniques for Yield Stress Analysis*; TA Instruments Tech. Notes-RH025; TA Instruments: New Castle, DE, USA, 2000; pp. 1–6.
29. Lin, Y.; Qin, H.; Guo, J.; Chen, J. Study on the rheological behavior of a model clay sediment. *J. Mar. Sci. Eng.* **2021**, *9*, 81. [[CrossRef](#)]

30. Barbosa, C.; Diogo, F.; Alves, M.R. Fitting mathematical models to describe the rheological behaviour of chocolate pastes. *AIP Conf. Proc.* **2016**, *1738*, 370016. [[CrossRef](#)]
31. Li, Z.; Guo, T.; Chen, Y.; Dong, L.; Chen, Q.; Hao, M.; Zhao, X.; Liu, J. Study on Rheological Properties of Graphene Oxide/Rubber Crowd Composite-Modified Asphalt. *Materials* **2022**, *2022*, 6185. [[CrossRef](#)]
32. Baudez, J.C.; Markis, F.; Eshtiaghi, N.; Slatter, P. The rheological behaviour of anaerobic digested sludge. *Water Res.* **2011**, *45*, 5675–5680. [[CrossRef](#)]
33. Hammadi, L.; Boudjenane, N.; Belhadri, M. Effect of polyethylene oxide (PEO) and shear rate on rheological properties of bentonite clay. *Appl. Clay Sci.* **2014**, *99*, 306–311. [[CrossRef](#)]
34. Beckett, S.T. *Industrial Chocolate*; Blackwell Publishing Ltd.: Hoboken, NJ, USA, 2009; ISBN 9781405139496.
35. Fischer, P.; Windhab, E.J. Rheology of food materials. *Curr. Opin. Colloid Interface Sci.* **2011**, *16*, 36–40. [[CrossRef](#)]
36. GARCIA, E.J.; STEFFE, J.F. Optimum Economic Pipe Diameter for Pumping Herschel-Bulkley Fluids in Laminar Flow. *J. Food Process Eng.* **1986**, *8*, 117–136. [[CrossRef](#)]

**Disclaimer/Publisher's Note:** The statements, opinions and data contained in all publications are solely those of the individual author(s) and contributor(s) and not of MDPI and/or the editor(s). MDPI and/or the editor(s) disclaim responsibility for any injury to people or property resulting from any ideas, methods, instructions or products referred to in the content.